Recalibration of the binding energy of hypernuclei measured in emulsion experiments and its implications*

Peng Liu(刘鹏)[1,2,3] Jinhui Chen(陈金辉)[4;1)] Declan Keane[5] Zhangbu Xu(许长补)[3,6] Yu-Gang Ma(马余刚)[1,4]

[1]Shanghai Institute of Applied Physics, Chinese Academy of Sciences, Shanghai 201800, China
[2]University of Chinese Academy of Sciences, Beijing 100049, China
[3]Brookhaven National Laboratory, Upton, New York 11973, USA
[4]Key Laboratory of Nuclear Physics and Ion-beam Application (MOE), Institute of Modern Physics, Fudan University, Shanghai 200433, China
[5]Kent State University, Kent, Ohio 44242, USA
[6]Shandong University, Qingdao, Shandong 266237, China

Abstract: The Λ separation energy for Λ hypernuclei, denoted B_Λ, measured in 1967, 1968, and 1973 are recalibrated using the current best estimates of the mass of particles and nuclei. The recalibrated B_Λ are systematically larger (except in the case of ${}^{6}_{\Lambda}$He) than the originally published values by about 100 keV. The effect of this level of recalibration is very important for light hypernuclei, especially for the hypertriton. The early B_Λ values measured in 1967, 1968, and 1973 are widely used in theoretical research, and the new results provide better constraints for the conclusions of such studies.

Keywords: hypernuclei, binding energy, recalibration

PACS: 21.80.+a, 21.10.k, 21.10.Dr **DOI:** 10.1088/1674-1137/43/12/124001

1 Introduction

A hypernucleus contains one or more strange quarks, and in the most common type of hypernucleus, a neutron is replaced by a Λ hyperon. The first hypernucleus was discovered by Marion Danysz and Jerzy Pniewski in 1952 in a balloon-flown emulsion plate [1]. Many other hypernuclei were observed during the following years in emulsion experiments [2, 3]. The hypertriton is the lightest hypernucleus, and is composed of a proton, a neutron, and a Λ hyperon. The antimatter partner of the hypertriton was discovered in a heavy ion collision experiment by the STAR collaboration at the Relativistic Heavy Ion Collider (RHIC) at Brookhaven National Laboratory in 2010 [4], and confirmed in 2015 by the ALICE collaboration at the Large Hadron Collider (LHC) at CERN [5]. The hyperon-nucleon (YN) interaction plays an important role in understanding the strong nuclear force [6, 7], and since hyperons may exist in the core of neutron stars [8], the YN interaction is also of importance for the study of neutron star properties [8-10]. Hyperon-nucleon scattering would be a good tool to explore the YN interaction, however it is very challenging to obtain stable hyperon beams due to the very short lifetime of the hyperon. Hypernuclei are a natural YN interaction system and thus their lifetime and binding energy have a direct connection to the strength of the YN interaction [11-13]. A precise determination of the hypernuclear lifetime and binding energy can serve as a critical input for theoretical studies of the strong force and neutron star interior [6-12, 14-16].

Although the data for hyperon-nucleon scattering is lacking, measurements of the Λ separation energy B_Λ for Λ hypernuclei have been available from the nuclear emulsion experiments [2, 3, 9, 17-20]. The separation energy B_Λ is defined as $(M_\Lambda + M_{\rm core} - M_{\rm hypernucleus})c^2$, where $M_{\rm hypernucleus}$, M_Λ and $M_{\rm core}$ are the mass of the hypernucleus, Λ hyperon, and of the nuclear core of the hypernucleus. The B_Λ measurements provided by emulsion experiments need to be revisited because the masses of particles and nuclei that were used in the original publications are different from the contemporary best estimates from PDG (Particle Data Group) [21] and AMDC (Atomic Mass Data Center, located at the Institute of Modern Physics, Chinese Academy of Sciences, Lanzhou) [22, 23]. A case in point is a recent improved measurement of B_Λ of the hypertriton, reported by the STAR collabora-

Received 14 August 2019, Published online 24 October 2019

* Supported by the Key Research Program of the Chinese Academy of Science (XDPB09), the National Natural Science Foundation of China (11890714, 11775288, 11421505, 11520101004), the China Scholarship Council (201704910615), the U.S. Department of Energy, Office of Science (DE-FG02-89ER40531, DE-SC-0012704)

1) E-mail: chenjinhui@fudan.edu.cn

tion in 2019 [24, 25], where the best estimate is significantly larger than the previous commonly cited value published in 1973 [20]. However, the early measurements of B_Λ have been used as critical input for theoretical research. For example, Ref. [11] applied the $\not\pi$EFT approach at LO to s-shell Λ hypernuclei with a precise few-body stochastic variational method to address the overbinding problem of ${}^{5}_{\Lambda}$He. In another relevant example, Ref. [10] considered two different models of three-body force constrained by the Λ separation energy of medium mass hypernuclei, but the authors obtained dramatically different results for the maximum mass of neutron stars using different models of the three-body force. Stronger constraints for the YN interaction are necessary to properly understand the role of hyperons in neutron stars. From this point of view, it is timely and highly desirable to recalibrate these early measurements using the contemporary best estimates of the mass of particles and nuclei [21-23], so as to provide more accurate constraints for contemporary studies [9, 11, 26, 27].

2 Techniques of recalibration

In the emulsion experiments, B_Λ was defined as [2, 3]:

$$B_\Lambda = Q_0 - Q, \tag{1}$$

$$Q_0 = M_{F'} + M_\Lambda - \sum_i M_i, \tag{2}$$

where Q is the total kinetic energy released when a hypernucleus decays through a mesonic decay channel, F' represents the nuclear core of the hypernucleus, M is the mass of a particle or nucleus, and the subscript i refers to the ith decay daughter. Q was determined using the range-energy relation in emulsions [2, 3, 18-20, 28], while Q_0 was directly determined from the masses of particles and nuclei available at the time of publication. A series of papers for nuclide masses was published at that time (in 1954 [29], 1960 [30, 31], 1962 [32], 1965 [33], 1971 [34], and 1977 [35]), and the nuclide masses published in 1960 [30, 31] were used in Ref. [17] for the B_Λ measurements. Ref. [17] is by the same corresponding author as Refs. [18-20], and we assume here that the masses used in 1967 [18] and 1968 [19] were taken from the nuclide mass paper published in 1965 [33]. We also assume that the masses used in 1973 [20] were taken from the nuclide mass paper published in 1971 [34]. The masses of π^-, proton, Λ, and the relevant nuclei used in the past and in 2019 are listed in Table 1. From Table 1, it is evident that the early masses of particles and nuclei are different from the current values. Consequently, the Q_0 values used in 1967, 1968, and 1973 were such that the original published B_Λ measurements were not as accurate as they could be. Fortunately, the early B_Λ values can be recalibrated by comparing the difference in Q_0 between the old publications and modern numbers. According to the masses listed in Table 1, Q_0 for light hypernuclei with mass number A = 3 - 15 is calculated for specific decay channels for the data from 1967, 1968, 1973 and 2019. Table 2 presents Q_0 and ΔQ_0, where the latter is the difference between Q_0 for 2019 and Q_0 in the specific earlier year. ΔQ_0 is used for recalibrating B_Λ measured in 1967, 1968 and 1973. The original B_Λ is recalibrated for each decay channel listed in Table 2. After recalibration, we provide more precise estimates of the B_Λ values. Table 3 lists the original and recalibrated B_Λ values for a combination of all available decay channels for the listed

Table 1. The masses of elementary particles and nuclei used in the past publications and in 2019. The nuclear masses used in 1967 and 1968 are taken from Refs. [29,30,33], those used in 1973 are taken from Ref. [34], while those used in 2019 are taken from Refs. [22,23]. All masses are in units of MeV/c^2.

Particle/ Nucleus	NPB1 (1967) [18]	NPB4 (1968) [19]	NPB52 (1973) [20]	2019
π^-	139.59 [17]	139.58 [40]	139.58 [41]	139.57 [21]
p	938.26 [17]	938.26 [40]	938.26 [41]	938.27 [21]
Λ	1115.44 [19]	1115.57 [19]	1115.57 [20]	1115.68 [21]
d	1875.51	1875.51	1875.63	1875.61
t	2808.76	2808.76	2808.95	2808.92
^{3}He	2808.23	2808.23	2808.42	2808.39
^{4}He	3727.17	3727.17	3727.42	3727.38
^{5}He	4667.64	4667.64	4667.89	4667.68
^{6}He	5605.22	5605.22	5605.60	5605.53
^{6}Li	5601.20	5601.20	5601.58	5601.52
^{6}Be	5604.97	5604.97	5605.35	5605.30
^{7}Li	6533.46	6533.46	6533.90	6533.83
^{7}Be	6533.81	6533.81	6534.25	6534.18
^{8}Li	7470.94	7470.94	7471.45	7471.36
^{8}Be	7454.43	7454.43	7454.93	7454.85
^{8}B	7471.90	7471.90	7472.40	7472.32
^{9}Be	8392.28	8392.28	8392.84	8392.75
^{9}B	8392.83	8392.83	8393.40	8393.31
^{10}Be	9324.97	9324.97	9325.60	9325.50
^{10}B	9323.91	9323.91	9324.54	9324.44
^{11}B	10251.96	10251.96	10252.66	10252.55
^{11}C	10253.43	10253.43	10254.13	10254.02
^{12}C	11174.23	11174.23	11174.98	11174.86
^{13}C	12108.79	12108.79	12109.61	12109.48
^{13}N	12110.50	12110.50	12111.32	12111.19
^{14}N	13039.46	13039.46	13040.34	13040.20
^{15}O	13970.39	13970.39	13971.33	13971.18

Table 2. The Q_0 and ΔQ_0 values for the year indicated at the top of each column. ΔQ_0 denotes Q_0 in 2019 minus Q_0 in the specified year. All Q_0 and ΔQ_0 values are in units of MeV/c^2.

Hypernucleus	Decay modes	NPB1 (1967) [18]		NPB4 (1968) [19]		NPB52 (1973) [20]		2019
		Q_0	ΔQ_0	Q_0	ΔQ_0	Q_0	ΔQ_0	Q_0
$^{3}_{\Lambda}$H	$\pi^- + {}^3$He	43.13	0.20	43.27	0.06	43.20	0.13	43.33
	$\pi^- + p + d$	37.59	0.25	37.73	0.11	37.73	0.11	37.84
$^{4}_{\Lambda}$H	$\pi^- + {}^4$He	57.44	0.21	57.58	0.07	57.52	0.13	57.65
	$\pi^- + p + t$	37.59	0.25	37.73	0.11	37.73	0.11	37.84
	$\pi^- + d + d$	33.59	0.22	33.73	0.08	33.68	0.13	33.81
^{4}He	$\pi^- + p + {}^3 + \mathrm{p} + {}^3$He	37.59	0.25	37.73	0.11	37.73	0.11	37.84
	$\pi^- + p + p + d$	32.05	0.30	32.19	0.16	32.26	0.09	32.35
$^{5}_{\Lambda}$He	$\pi^- + p + {}^4$He	37.59	0.25	37.73	0.11	37.73	0.11	37.84
	$\pi^- + d + {}^3$He	19.28	0.21	19.42	0.07	19.36	0.13	19.49
	$\pi^- + p + p + t$	17.74	0.29	17.88	0.15	17.94	0.09	18.03
	$\pi^- + p + d + d$	13.74	0.26	13.88	0.12	13.89	0.11	14.00
$^{6}_{\Lambda}$He	$\pi^- + d + {}^4$He	40.81	−0.01	40.95	−0.15	40.83	−0.03	40.80
$^{7}_{\Lambda}$He	$\pi^- + {}^7$Li	47.61	0.20	47.75	0.06	47.69	0.12	47.81
	$\pi^- + p + {}^6\mathrm{He} + {}^6$He	37.59	0.25	37.73	0.11	37.73	0.11	37.84
	$\pi^- + t + {}^4$He	45.14	0.20	45.28	0.06	45.22	0.12	45.34
	$\pi^- + p + t + t$	25.29	0.24	25.43	0.10	25.43	0.10	25.53
$^{7}_{\Lambda}$Li	$\pi^- + p + {}^6$Li	37.59	0.25	37.73	0.11	37.73	0.11	37.84
	$\pi^- + {}^3\mathrm{He} + {}^4$He	41.65	0.21	41.79	0.07	41.73	0.13	41.86
	$\pi^- + p + d + {}^4$He	36.11	0.26	36.25	0.12	36.26	0.11	36.37
$^{7}_{\Lambda}$Be	$\pi^- + p + p + p + {}^4$He	38.87	0.35	39.01	0.21	39.14	0.08	39.22
$^{8}_{\Lambda}$Li	$\pi^- + {}^4\mathrm{He} + {}^4$He	54.97	0.21	55.11	0.07	55.05	0.13	55.18
	$\pi^- + p + t + {}^4$He	35.12	0.25	35.26	0.11	35.26	0.11	35.37
	$\pi^- + d + d + {}^4$He	31.12	0.22	31.26	0.08	31.21	0.13	31.34
	$\pi^- + d + {}^6\mathrm{Li} + {}^6$Li	32.60	0.21	32.74	0.07	32.68	0.13	32.81
$^{8}_{\Lambda}$Be	$\pi^- + {}^8$B	37.76	0.21	37.90	0.07	37.84	0.13	37.97
	$\pi^- + p + {}^7$Be	37.59	0.25	37.73	0.11	37.73	0.11	37.84
	$\pi^- + p + {}^3\mathrm{He} + {}^4$He	36.00	0.25	36.14	0.11	36.14	0.11	36.25
	$\pi^- + p + p + {}^6$Li	31.94	0.29	32.08	0.15	32.14	0.09	32.23
	$\pi^- + p + p + d + {}^4$He	30.46	0.30	30.60	0.16	30.67	0.09	30.76
$^{9}_{\Lambda}$Li	$\pi^- + {}^9$Be	54.51	0.21	54.65	0.07	54.60	0.12	54.72
	$\pi^- + p + {}^8$Li	37.59	0.25	37.73	0.11	37.73	0.11	37.84
	$\pi^- + t + {}^6$Li	36.83	0.20	36.97	0.06	36.91	0.12	37.03
$^{9}_{\Lambda}$Be	$\pi^- + {}^9$B	37.45	0.20	37.59	0.06	37.52	0.13	37.65
	$\pi^- + p + {}^4\mathrm{He} + {}^4$He	37.68	0.25	37.82	0.11	37.82	0.11	37.93
$^{9}_{\Lambda}$B	$\pi^- + p + {}^8$B	37.59	0.25	37.73	0.11	37.73	0.11	37.84
	$\pi^- + p + p + p + {}^6$Li	31.77	0.33	31.91	0.19	32.03	0.07	32.10
$^{10}_{\Lambda}$Be	$\pi^- + p + p + {}^8$Li	20.67	0.29	20.81	0.15	20.86	0.10	20.96
$^{10}_{\Lambda}$B	$\pi^- + p + {}^9$B	37.59	0.25	37.73	0.11	37.73	0.11	37.84
	$\pi^- + p + p + {}^4\mathrm{He} + {}^4$He	37.82	0.30	37.96	0.16	38.03	0.09	38.12

Continued on next page

Table 2-continued from previous page

Hypernucleus	Decay modes	NPB1 (1967) [18]		NPB4 (1968) [19]		NPB52 (1973) [20]		2019
		Q_0	ΔQ_0	Q_0	ΔQ_0	Q_0	ΔQ_0	Q_0
$^{11}_{\Lambda}$B	$\pi^- + {}^{11}$C	46.33	0.20	46.47	0.06	46.40	0.13	46.53
	$\pi^- + p + d + {}^4$He + ^{4}He	31.65	0.26	31.79	0.12	31.80	0.11	31.91
	$\pi^- + {}^4$He + ^{7}Be	38.78	0.21	38.92	0.07	38.86	0.13	38.99
	$\pi^- + {}^3$He + ^{4}He + ^{4}He	37.19	0.21	37.33	0.07	37.27	0.13	37.40
	$\pi^- + p + {}^4$He + ^{6}Li	33.13	0.25	33.27	0.11	33.27	0.11	33.38
	$\pi^- + t + {}^8$B	19.10	0.21	19.24	0.07	19.18	0.13	19.31
$^{12}_{\Lambda}$B	$\pi^- + {}^4$He + ^{4}He + ^{4}He	46.30	0.22	46.44	0.08	46.39	0.13	46.52
$^{13}_{\Lambda}$C	$\pi^- + {}^{13}$N	39.58	0.20	39.72	0.06	39.65	0.13	39.78
	$\pi^- + p + {}^4$He + ^{4}He + ^{4}He	30.31	0.25	30.45	0.11	30.45	0.11	30.56
$^{15}_{\Lambda}$N	$\pi^- + {}^{15}$O	44.92	0.21	45.06	0.07	45.00	0.13	45.13

Table 3. The original and the recalibrated Λ separation energy for hypernuclei data from 1967 [18], 1968 [19], and 1973 [20]. The listed errors are the reported statistical uncertainties only, and the recalibrated Λ separation energy should be considered as subject to the same errors as the original measurements. The Λ separation energy is in units of MeV.

Hypernucleus	NPB1 (1967) [18]		NPB4 (1968) [19]		NPB52 (1973) [20]	
	Original	Recalibrated	Original	Recalibrated	Original	Recalibrated
$^{3}_{\Lambda}$H	0.20 ± 0.12	0.41	0.01 ± 0.07	0.08	0.15 ± 0.08	0.27
$^{4}_{\Lambda}$H	2.13 ± 0.06	2.35	2.23 ± 0.03	2.31	2.08 ± 0.06	2.20
$^{4}_{\Lambda}$He	2.20 ± 0.06	2.45	2.36 ± 0.04	2.47	2.42 ± 0.04	2.53
$^{5}_{\Lambda}$He	3.08 ± 0.03	3.33	3.08 ± 0.02	3.19	3.17 ± 0.02	3.28
$^{6}_{\Lambda}$He	4.09 ± 0.27	4.08	4.38 ± 0.19	4.23	4.42 ± 0.13	4.39
$^{7}_{\Lambda}$He	4.67 ± 0.28	4.88	4.25 ± 0.25	4.34	No data	No data
$^{7}_{\Lambda}$Li	5.46 ± 0.12	5.68	5.60 ± 0.07	5.67	5.64 ± 0.04	5.77
$^{7}_{\Lambda}$Be	5.36 ± 0.23	5.71	5.06 ± 0.19	5.27	5.09 ± 0.11	5.17
$^{8}_{\Lambda}$Li	6.72 ± 0.08	6.93	6.84 ± 0.06	6.91	6.81 ± 0.03	6.94
$^{8}_{\Lambda}$Be	6.67 ± 0.16	6.89	6.87 ± 0.08	6.95	6.91 ± 0.07	7.02
$^{9}_{\Lambda}$Li	8.27 ± 0.18	8.49	8.23 ± 0.19	8.34	8.59 ± 0.17	8.70
$^{9}_{\Lambda}$Be	6.66 ± 0.08	6.88	6.62 ± 0.05	6.68	6.80 ± 0.03	6.93
$^{9}_{\Lambda}$B	No data	No data	No data	No data	7.89 ± 0.15	7.98
$^{10}_{\Lambda}$Be	No data	No data	No data	No data	9.30 ± 0.26	9.40
$^{10}_{\Lambda}$B	No data	No data	No data	No data	8.82 ± 0.12	8.93
$^{11}_{\Lambda}$B	10.30 ± 0.14	10.51	9.99 ± 0.18	10.11	10.24 ± 0.06	10.37
$^{12}_{\Lambda}$B	11.26 ± 0.16	11.48	10.95 ± 0.16	11.03	11.45 ± 0.07	11.58
$^{13}_{\Lambda}$C	10.51 ± 0.51	10.71	No data	No data	11.45 ± 0.12	11.57
$^{15}_{\Lambda}$N	No data	No data	No data	No data	13.59 ± 0.14	13.72

Λ hypernuclei with mass numbers A = 3-15.

We note that the early emulsion measurements from 1968 and 1973 benefited from a compensating effect in normalizing the B_{Λ} values to the measured mass of the Λ hyperon with the decay daughter π^- range of 1-2 cm in the same emulsion stack [19, 20]. Because the mass of Λ hyperon and Q appear with opposite signs in Eq. (1), it was argued that the systematic errors arising from the uncertainties in both the range-energy relation and the emulsion density are largely offset by the normalization procedure, and a small systematic error of 0.04 MeV was determined for the early measurements [19, 20, 36-38]. Although an identical Λ mass was measured in 1968 and 1973, the differences of B_Λ between measurements in these two years are large (up to 0.50 ± 0.17 (stat.) MeV [20]), which is significantly larger than the systematic error of 0.04 MeV. The ranges of π^- from Λ decays in the emulsion experiments were chosen to be 1-2 cm, a range interval that covers the majority of π^- from hypernuclear decays. Nevertheless, the distribution of π^- ranges from Λ decay and hypernuclear decay were different [19, 20, 28]. This difference in π^- range can also yield a difference in the measured Q value as large as 0.43 ± 0.13 (stat.) MeV [28], and cannot ensure that the deviations of measured Q values for Λ decay and hypernuclear decay are in the same direction [28]. Recent precise measurements show that for p-shell hypernuclei, there is a discrepancy in the range of 0.4-0.8 MeV between the early emulsion measurements and the recent data [39]. The authors of Ref. [39] also argue that the emulsion data significantly underestimated the systematic error, which is dependent on the specific hypernucleus. Based on the above statement, we believe that the compensating effect described above may not fully account for the systematic errors, and a recalibration of the Q_0 differences seems to be a more reliable method.

3 Results and discussion

We note that it is tempting to average the recalibrated early measurements for each hypernucleus to obtain a more precise best value. However, as explained above, without a better understanding of systematic uncertainties associated with emulsion measurements, it is not appropriate to perform a weighted average. From Table 3, it is evident that the recalibrated B_Λ values are systematically larger than the original estimates, except in the case of ${}^{6}_{\Lambda}$He. Compared with the original ${}^{3}_{\Lambda}$H $B_\Lambda = 0.13\pm0.05$(stat.) MeV, which was published in 1973 and widely used in modern theoretical studies, the recalibrated $B_\Lambda = 0.27\pm0.08$(stat.) MeV is closer to the latest result, namely $B_\Lambda = 0.41\pm0.12$(stat.)±0.11(syst.) MeV, published by the STAR collaboration in 2019 [24, 25]. The latest precise measurement of ${}^{4}_{\Lambda}$H by the A1 collaboration in 2016 is 2.157 ± 0.005 (stat.) ± 0.077 (syst.) MeV [42], which is also closer to our recalibrated value when compared with the original values presented in 1973. In addition, in contrast to the original emulsion measurements, our recalibrated values for ${}^{7}_{\Lambda}$He and ${}^{7}_{\Lambda}$Li are also closer to the latest measurement $B_\Lambda({}^{7}_{\Lambda}\mathrm{He}) = 5.55\pm0.10$(stat.)$\pm0.11$ (syst.) MeV by the HKS collaboration in 2016 [43] , and $B_\Lambda({}^{7}_{\Lambda}\mathrm{Li}) = 5.85\pm0.13$,(stat.)$\pm$ 0.11(syst.) MeV by the FINUDA collaboration in 2009 [44, 45] . These numbers corroborate the expectation that all recalibrated B_Λ values presented in this paper are indeed better estimates than the early measurements in the light hypernuclei region. In recent years, collaborations at Jefferson Lab and the DAΦNE-FINUDA collaboration measured B_Λ with good accuracy for heavier hypernuclei, namely $B_\Lambda({}^{9}_{\Lambda}\mathrm{Li})$ =8.36±0.08 (stat.)±0.08(syst.) MeV [46], $B_\Lambda({}^{9}_{\Lambda}\mathrm{Be})$ =6.30±0.10(stat.)± 0.10(syst.) MeV [44, 45], $B_\Lambda({}^{10}_{\Lambda}\mathrm{Be})$ =8.60±0.07(stat.)±0.16 (syst.) MeV [47], $B_\Lambda({}^{11}_{\Lambda}\mathrm{B})$=10.28±0.2(stat.)±0.4(syst.) MeV [44], $B_\Lambda({}^{12}_{\Lambda}\mathrm{B})$ = 11.524±0.019 (stat.)±0.013 (syst.) MeV [48], $B_\Lambda({}^{13}_{\Lambda}\mathrm{C})$ = 11.0±0.4 MeV [49], and $B_\Lambda({}^{15}_{\Lambda}\mathrm{N})$ = 13.8±0.7(stat.)±1.0 (syst.) MeV [44]. Comparing these measurements with the early emulsion measurements, some recent results indicate larger B_Λ. However, some of them show smaller B_Λ.

The recalibrated Λ separation energy B_Λ of hypernuclei from 1973 (except for ${}^{7}_{\Lambda}$He, whose value dates from 1968) along with the values [9] for hypernuclei with the mass number $A > 15$ are collected in Figs. 1, 2, and 3. Figure 1 shows B_Λ as a function of the hypernuclear mass number A. From Fig. 1, it is evident that B_Λ dramatically increases with mass number up to about $A \sim 15$. As A becomes larger, B_Λ increases more slowly and indicates a trend towards saturation in the limit of very large A. As shown in the right panel of Fig. 1, a straight line provides a good fit to the recalibrated B_Λ in the region of light hypernuclei, i.e., $A < 15$.

Figure 2 shows the strength of the interaction between a nucleon in the core of a hypernucleus and the bound Λ. From Fig. 2, it is evident that the strength of the interaction between a nucleon and Λ first dramatically increases with A, and then decreases. At very large A, it shows a tendency to flatten out. From the right panel of Fig. 2, it is evident that $B_\Lambda/(A-1)$ reaches a maximum between $A = 8$ and $A = 12$. Fig. 3 presents B_Λ versus $A^{-2/3}$. The dashed black curve is the solution of the Schrödinger equation with the standard Woods-Saxon potential [9], which describes the medium and heavy mass range. A semi-empirical formula based on the Fermi gas model is also employed for B_Λ of light, medium, and heavy hypernuclei [50], as shown in Fig. 3. Although this semi-empirical formula shows good agreement in the mid-mass range, it is not good enough for fitting the experimental data in the light and heavy mass range. On the other hand, the Woods-Saxon potential and the semi-empirical formula do not take into account the Charge Symmetry Breaking (CSB) effect. The right panel of Fig. 3 is a zoom of the region $A \leqslant 7$, where the theoretical calculations span a wide range, as shown in the right panel of Fig. 3 , and consequently our recalibration becomes more important.

The recalibrated values are systematically larger (except in the case of ${}^{6}_{\Lambda}$He) than the original values by about 100 keV, which is mainly due to the difference of the Λ

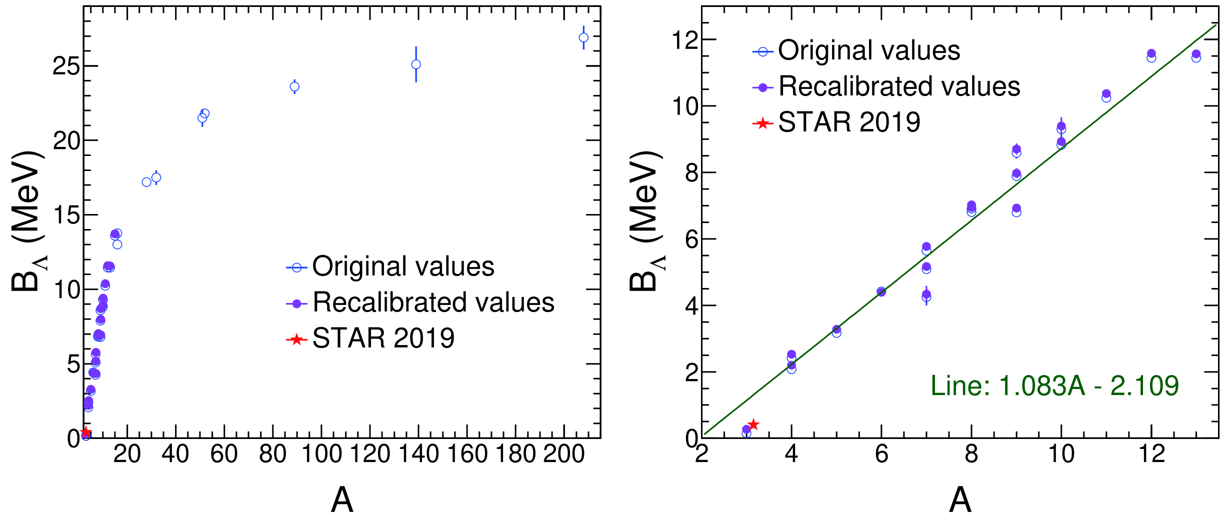

Fig. 1. (color online) The Λ separation energy B_Λ of hypernuclei as a function of the mass number A. The original and the recalibrated values are shown together with the latest measurement for the hypertriton by the STAR collaboration [24]. The error bars are the reported uncertainties. The caps and error bar shown for the STAR measurement are the systematic and statistical uncertainty, respectively. The right panel shows a magnified view. The STAR point is moved away from A = 3 to make it visible. A straight line is fitted to the recalibrated values in the range A = 3 -15. The green line and the green text shown in this figure are the fit results.

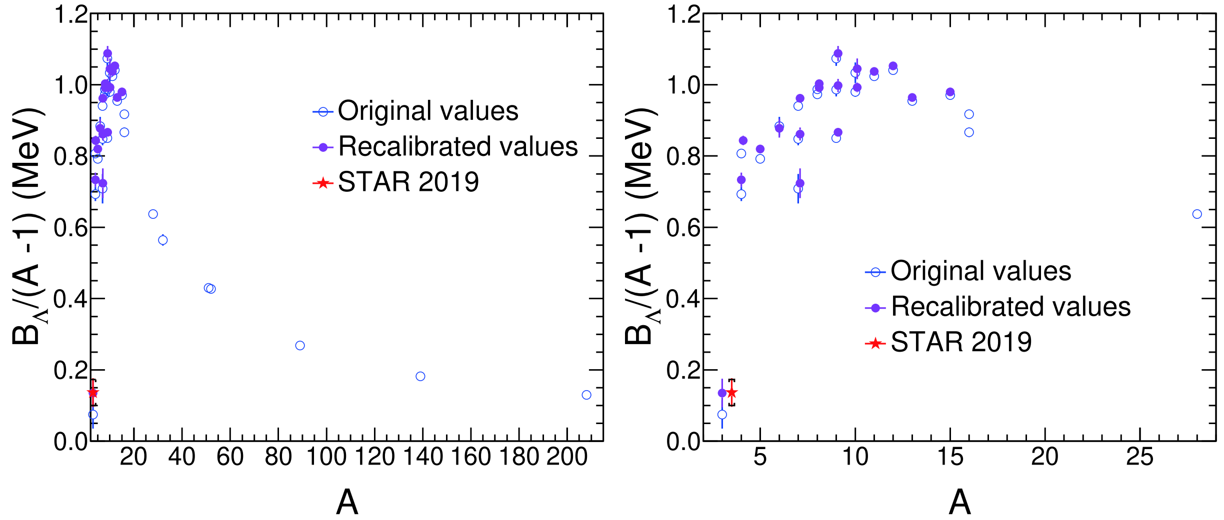

Fig. 2. (color online) The hypernuclear Λ separation energy B_Λ per baryon in the core of hypernuclei as a function of the mass number A. The original and the recalibrated values are shown together with the latest measurement for the hypertriton by the STAR collaboration [24]. The error bars are the reported uncertainties. The caps and error bar shown for the STAR measurement are the systematic and statistical uncertainty, respectively. The right panel shows a magnified view. The STAR point is displaced slightly from $A = 3$ for visibility.

hyperon mass between the modern and the early emulsion values. This effect is more significant for light hypernuclei, especially for $^{3}_{\Lambda}$H, since its B_Λ is very small compared with heavy hypernuclei. These larger B_Λ of light hypernuclei obtained by recalibrating the emulsion data and from the recent experimental measurements will help to understand the puzzle of reduced lifetime of $^{3}_{\Lambda}$H [51]. The latest compilation of measurements yields a $^{3}_{\Lambda}$H lifetime shorter than the free Λ lifetime [13, 52]. A calculation in which the closure approximation was introduced to evaluate the wave functions by solving the three-body Faddeev equations, indicates that the $^{3}_{\Lambda}$H lifetime is (19 ± 2)% smaller than that of Λ [53]. The shorter lifetime is consistent with a larger Λ separation energy in $^{3}_{\Lambda}$H. The significant change in B_Λ of $^{3}_{\Lambda}$H will also improve the understanding of other hypernuclei [11]. We also see from Table 3 that B_Λ for hypernuclei with the same mass number A but different electric charge are sig-

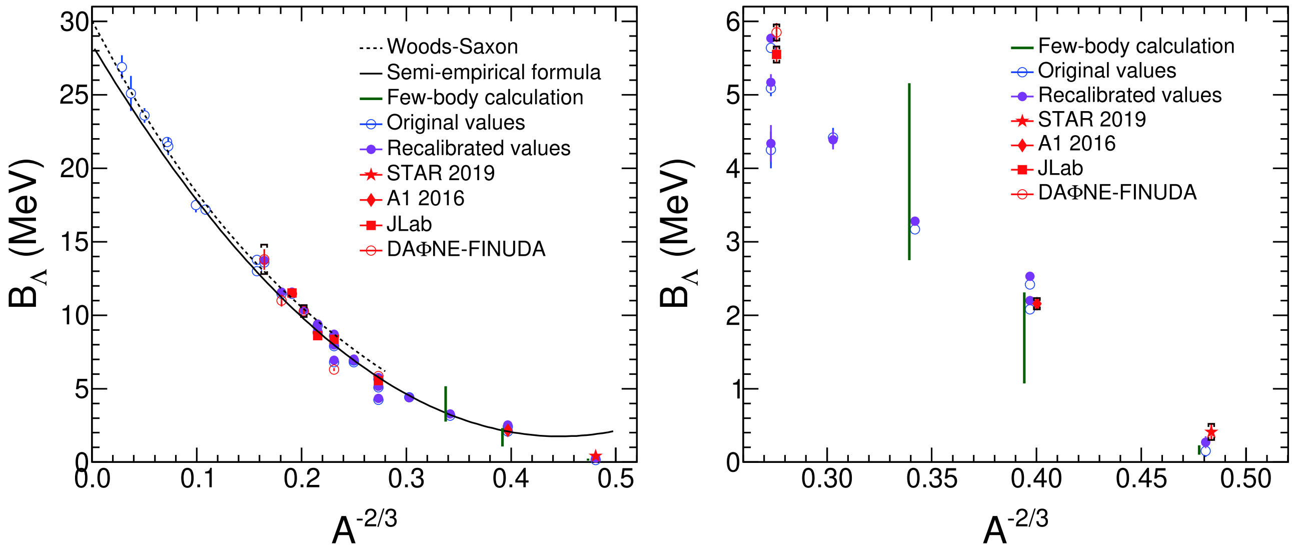

Fig. 3. (color online) The hypernuclear Λ separation energy B_Λ as a function of $A^{-2/3}$. The original and the recalibrated values are shown together with the latest measurement for $^{3}_{\Lambda}$H by the STAR collaboration [24], the measurement for $^{4}_{\Lambda}$H by the A1 collaboration [42], the measurements for $^{7}_{\Lambda}$He, $^{9}_{\Lambda}$Li, $^{10}_{\Lambda}$Be, and $^{12}_{\Lambda}$B by JLab [43, 46-48], and the measurements for $^{7}_{\Lambda}$Li, $^{9}_{\Lambda}$Be, $^{11}_{\Lambda}$B, $^{13}_{\Lambda}$C, and $^{15}_{\Lambda}$N by the DAΦNE-FINUDA collaboration [44, 45, 49]. The error bars are the reported uncertainties. The caps and error bars shown for the STAR, A1, JLab, and DAΦNE-FINUDA measurements are the systematic and statistical uncertainty, respectively. The dashed black curve in the left panel was obtained by solving the Schrödinger equation with the standard Woods-Saxon potential [9], and the solid black curve is a semi-empirical formula [50]. The green vertical lines near the experimental points are several representative few-body calculations [11, 27]. The right panel shows a magnified view, where the markers for STAR, A1, JLab, and DAΦNE-FINUDA are displaced slightly from their corresponding mass numbers for visiblity.

Table 4. Comparison between the Λ separation energy (B_Λ) for each listed hypernucleus and the binding energy of the last neutron (S_n) and proton (S_p) in the corresponding nucleus with the same A and Z. The B_Λ values for hypernuclei with $A \leqslant 15$ are the recalibrated B_Λ from 1973 (except for $^{7}_{\Lambda}$He, where the recalibrated 1968 data is used), while the data for hypernuclei with $A > 15$ are from Ref. [9]. The S_n and S_p values are taken from the database maintained by the International Atomic Energy Agency (IAEA) [54]. B_Λ, S_n and S_p are in units of MeV.

	$^{3}_{\Lambda}$H (t)	$^{4}_{\Lambda}$He (^{4}He)	$^{5}_{\Lambda}$He (^{5}He)	$^{6}_{\Lambda}$He (^{6}He)	$^{7}_{\Lambda}$He (^{7}He)	$^{7}_{\Lambda}$Li (^{7}Li)	$^{7}_{\Lambda}$Be (^{7}Be)
B_Λ	0.27 ± 0.08	2.53 ± 0.04	3.28 ± 0.02	4.39 ± 0.13	4.34 ± 0.25	5.77 ± 0.04	5.17 ± 0.11
S_n	6.26	20.58	−0.74 ± 0.02	1.71 ± 0.02	−0.41 ± 0.01	7.25	10.68
S_p	No data	19.81	20.68 ± 0.10	22.59 ± 0.09	23.09 ± 0.25	9.97	5.61
	$^{8}_{\Lambda}$Li (^{8}Li)	$^{8}_{\Lambda}$Be (^{8}Be)	$^{9}_{\Lambda}$Li (^{9}Li)	$^{9}_{\Lambda}$Be (^{9}Be)	$^{9}_{\Lambda}$B (^{9}B)	$^{10}_{\Lambda}$Be (^{10}Be)	$^{10}_{\Lambda}$B (^{10}B)
B_Λ	6.94 ± 0.03	7.02 ± 0.07	8.70 ± 0.17	6.93 ± 0.03	7.98 ± 0.15	9.40 ± 0.26	8.93 ± 0.12
S_n	2.03	18.90	4.06	1.66	18.58	6.81	8.44
S_p	12.42	17.25	13.94	16.89	−0.19	19.64	6.59
	$^{11}_{\Lambda}$B (^{11}B)	$^{12}_{\Lambda}$B (^{12}B)	$^{13}_{\Lambda}$C (^{13}C)	$^{15}_{\Lambda}$N (^{15}N)	$^{16}_{\Lambda}$N (^{16}N)	$^{16}_{\Lambda}$O (^{16}O)	$^{28}_{\Lambda}$Si (^{28}Si)
B_Λ	10.37 ± 0.06	11.58 ± 0.07	11.57 ± 0.12	13.72 ± 0.14	13.76 ± 0.16	13.0 ± 0.2	17.2 ± 0.2
S_n	11.45	3.37	4.95	10.83	2.49	15.66	17.18
S_p	11.23	14.10	17.53	10.21	11.48	12.13	11.58
	$^{32}_{\Lambda}$S (^{32}S)	$^{51}_{\Lambda}$V (^{51}V)	$^{52}_{\Lambda}$V (^{52}V)	$^{89}_{\Lambda}$Y (^{89}Y)	$^{139}_{\Lambda}$La (^{139}La)	$^{208}_{\Lambda}$Pb (^{208}Pb)	
B_Λ	17.5 ± 0.5	21.5 ± 0.6	21.8 ± 0.3	23.6 ± 0.5	25.1 ± 1.2	26.9 ± 0.8	
S_n	15.04	11.05	7.31	11.48	8.78	7.37	
S_p	8.86	8.06	9.00	7.08	6.25	8.00	

nificantly different, i.e., the CSB effect [44]. Theoretical studies are particularly needed to address the CSB effect.

We also investigate the difference between B_Λ of hypernuclei and the corresponding binding energy of the last neutron and proton (S_n and S_p) of ordinary nuclei, as shown in Table 4. B_Λ increases with A, but S_n and S_p show a significantly different behavior. This difference means that a Λ hyperon plays a different role in a nucleus than a nucleon. On the other hand, this difference may be related to the rich structure of the nuclear core. For example, the Gaussian expansion method provides an accurate structure calculation of light hypernuclei by treating them as three and/or four clusters [55].

4 Summary

In summary, the early measurements of the Λ separation energy B_Λ for Λ hypernuclei published in 1967, 1968, and 1973 were recalibrated with the current most accurate values of the mass of particles and nuclei. The recalibrated B_Λ are systematically larger (except in the case of $^{6}_{\Lambda}$He) than the original published values by about 100 keV. The effect of this level of recalibration is most significant for light hypernuclei, especially for the hypertriton. Our recalibrated B_Λ give rise to new constraints for the theoretical studies of the strong force, the structure of hypernuclei, and neutron star interior. Although this paper provides better B_Λ estimates by recalibrating the early measurements using modern masses of particles and nuclei, the latter may also suffer from significant systematic uncertainties, such as from the energy-range relation in an emulsion and the emulsion density [28, 38, 44, 56]. To further improve the constraints for theoretical research, more precise measurements of the fundamental properties of hypernuclei, like the mass and binding energy, are highly desirable. More precise measurements can be expected in the near future as a result of the on-going phase-II of the Beam Energy Scan program at RHIC, the high resolution spectroscopic experiments at Jefferson Lab [57] in the US, and the experiments at the Mainz Microton (MAMI) in Germany, while further progress will be made possible by measurements at the High Intensity Accelerator Facility (HIAF) under construction in China [58], at the Facility for Antiproton and Ion Research (FAIR) under construction in Germany, at the Japan Proton Accelerator Research Complex (J-PARC), and at the Nuclear Spectroscopic Telescope Array (NuSTAR) in the US.

We thank Prof. John Millener for insightful discussions and for sharing with us the private communication with Prof. Don Davis and the Woods-Saxon potential data.

References

1 M. Danysz and J. Pniewski, The London, Edinburgh, and Dublin Philosophical Magazine and Journal of Science, **44**: 348-350 (1953)
2 R. Levi-Setti, W. E. Slater, and V. L. Telegdi, Il Nuovo Cimento Series 10, **10**: 68-90 (1958)
3 E. M. Silverstein, Il Nuovo Cimento Series 10, **10**: 41-67 (1958)
4 B. I. Abelev et al (STAR Collaboration), Science, **328**: 58-62 (2010)
5 J. Adam et al (ALICE Collaboration), Phys. Lett. B, **754**: 360-372 (2016)
6 E. Botta, T. Bressani, and G. Garbarino, Eur. Phys. J. A, **48**: 41 (2012)
7 H. Müller and J. R. Shepard, J. Phys. G: Nucl. Part. Phys., **26**: 1049-1064 (2000)
8 D. Chatterjee and I. Vidaña, Eur. Phys. J. A, **52**: 29 (2016)
9 A. Gal, E. V. Hungerford, and D. J. Millener, Rev. Mod. Phys., **88**: 035004 (2016)
10 D. Lonardoni, A. Lovato, S. Gandolfi et al, Phys. Rev. Lett., **114**: 092301 (2015)
11 L. Contessi, N. Barnea, and A. Gal, Phys. Rev. Lett., **121**: 102502 (2018)
12 S. R. Beane, E. Chang, S. D. Cohen et al, Phys. Rev. D, **87**: 034506 (2013)
13 L. Adamczyk et al (STAR Collaboration), Phys. Rev. C, **97**: 054909 (2018)
14 J. M. Lattimer and M. Prakash, Science, **304**: 536-542 (2004)
15 M. Fortin, S. S. Avancini, C. Providência et al, Phys. Rev. C, **95**: 065803 (2017)
16 Jinhui Chen, Declan Keane, Yu-Gang Ma et al, Phys. Rep., **760**: 1-39 (2018)
17 C. Mayeur, J. Sacton, P. Vilain et al, Il Nuovo Cimento A (1971-1996), **43**: 180-192 (1966)
18 W. Gajewski, C. Mayeur, J. Sacton et al, Nucl. Phys. B, **1**: 105-113 (1967)
19 G. Bohm, J. Klabuhn, U. Krecker et al, Nucl. Phys. B, **4**: 511-526 (1968)
20 M. Juric, G. Bohm, J. Klabuhn et al, Nucl. Phys. B, **52**: 1-30 (1973)
21 M. Tanabashi et al (Particle Data Group), Phys. Rev. D, **98**: 030001 (2018)
22 W. J. Huang, G. Audi, M. Wang et al, Chin. Phys. C, **41**: 030002 (2017)
23 M. Wang, G. Audi, F. G. Kondev et al, Chin. Phys. C, **41**: 030003 (2017)
24 J. Adam et al (STAR Collaboration), arXiv: 1904.10520
25 Peng Liu (for the STAR Collaboration), Nucl. Phys. A, **982**: 811-814 (2019)
26 D. Lonardoni, F. Pederiva, and S. Gandolfi, Phys. Rev. C, **89**: 014314 (2014)
27 D. Lonardoni and F. Pederiva, arXiv: 1711.07521
28 G. Bohm, U. Krecker, C. Mayeur et al, Nuovo Cimento A (1965-1970), **70**: 384-390 (1970)
29 A. H. Wapstra, Physica, **21**: 367-384 (1954)
30 F. Everling, L. A. König, J. H. E. Mattauch et al, Nucl. Phys., **15**: 342-355 (1960)
31 F. Everling, L. A. König, J. H. E. Mattauch et al, Nucl. Phys., **18**: 529-569 (1960)
32 L. A. König, J. H. E. Mattauch, and A. H. Wapstra, Nucl. Phys., **31**: 18-42 (1962)
33 J. H. E. Mattauch, W. Thiele, and A. H. Wapstra, Nucl. Phys., **67**:

1-31 (1965)
34 A. H. Wapstra and N. B. Gove, At. Data Nucl. Data Tables, **9**: 267-301 (1971)
35 A. H. Wapstra and K. Bos, At. Data Nucl. Data Tables, **19**: 177-214 (1977)
36 D. H. Davis, Contemp. Phys., **27**: 91-116 (1986)
37 D. H. Davis, Nucl. Phys. A, **547**: 369c-378c (1992)
38 D. H. Davis, Nucl. Phys. A, **754**: 3-13 (2005)
39 P. Achenbach, S. Bleser, J. Pochodzalla et al, PoS, **Hadron2017**: 207 (2018)
40 A. H. Rosenfeld, A. Barbaro-Galtieri, W. J. Podolsky et al, Rev. Mod. Phys., **39**: 1-51 (1967)
41 N. Barash-Schmidt et al (Particle Data Group), http://pdg.lbl.gov/rpp-archive/files/cm-p00040028.pdf, retrieved 5th August 2019
42 F. Schulz et al (A1 Collaboration), Nucl. Phys. A, **954**: 149-160 (2016)
43 T. Gogami et al (HKS (JLab E05-115) Collaboration), Phys. Rev. C, **94**: 021302 (2016)
44 E. Botta, T. Bressani, and A. Feliciello, Nucl. Phys. A, **960**: 165-179 (2017)
45 M. Agnello et al (FINUDA Collaboration), Phys. Lett. B, **681**: 139-146 (2009)
46 G. M. Urciuoli et al (Jefferson Lab Hall A Collaboration), Phys. Rev. C, **91**: 034308 (2015)
47 T. Gogami et al (HKS (JLab E05-115) Collaboration), Phys. Rev. C, **93**: 034314 (2016)
48 L. Tang et al (HKS (JLab E05-115 and E01-011) Collaborations), Phys. Rev. C, **90**: 034320 (2014)
49 M. Agnello et al, Phys. Lett. B, **698**: 219-225 (2011)
50 K. P. Santhosh and C. Nithya, Eur. Phys. Plus J., **133**: 343 (2018)
51 J.-M. Richard, Q. Wang, and Q. Zhao, arXiv: 1604.04208v1
52 S. Acharya et al (ALICE Collaboration), arXiv: 1907.06906
53 A. Gal and H. Garcilazo, Phys. Lett. B, **791**: 48-53 (2019)
54 Nuclear Data Services of International Atomic Energy Agency (IAEA), https://www-nds.iaea.org/, retrieved 5th August 2019
55 E. Hiyama and T. Yamada, Prog. Part. Nucl. Phys., **63**: 339-395 (2009)
56 Private communication with Prof. D. J. Millener and Prof. D. H. Davis
57 S. N Nakamura, T. Gogami, and L. Tang (for the JLab hypernuclear Collaboration), JPS Conf. Proc., **17**: 011002 (2017)
58 Peng Liu, Jin-Hui Chen, Yu-Gang Ma et al, Nucl. Sci. Tech., **28**: 55 (2017)